RADIATION RESEARCH **166**, 141–157 (2006)
0033-7587/06 $15.00

Dose Reconstruction for Therapeutic and Diagnostic Radiation Exposures: Use in Epidemiological Studies

Marilyn Stovall,[a,1] Rita Weathers,[a] Catherine Kasper,[a] Susan A. Smith,[a] Lois Travis,[b] Elaine Ron[b] and Ruth Kleinerman[b]

[a] *Department of Radiation Physics, The University of Texas M. D. Anderson Cancer Center, Houston, Texas and* [b] *Division of Cancer Epidemiology and Genetics, National Cancer Institute, National Institutes of Health, Department of Health and Human Services, Rockville, Maryland*

Stovall, M., Weathers, R., Kasper, C., Smith, S. A., Travis, L., Ron, E. and Kleinerman, R. Dose Reconstruction for Therapeutic and Diagnostic Radiation Exposures: Use in Epidemiological Studies. *Radiat. Res.* 166, 141–157 (2006).

This paper describes methods developed specifically for reconstructing individual organ- and tissue-absorbed dose of radiation from past exposures from medical treatments and procedures for use in epidemiological studies. These methods have evolved over the past three decades and have been applied to a variety of medical exposures including external-beam radiation therapy and brachytherapy for malignant and benign diseases as well as diagnostic examinations. The methods used for estimating absorbed dose to organs in and outside the defined treatment volume generally require archival data collection, abstraction and review, and phantom measurements to simulate past exposure conditions. Three techniques are used to estimate doses from radiation therapy: (1) calculation in three-dimensional mathematical computer models using an extensive database of out-of-beam doses measured in tissue-equivalent materials, (2) measurement in anthropomorphic phantoms constructed of tissue-equivalent material, and (3) calculation using a three-dimensional treatment-planning computer. For diagnostic exposures, doses are estimated from published data and software based on Monte Carlo techniques. We describe and compare these methods of dose estimation and discuss uncertainties in estimated organ doses and potential for future improvement. Seven epidemiological studies are discussed to illustrate the methods.

INTRODUCTION

Patients exposed to radiation during treatment for malignant and benign diseases and for diagnostic purposes are well suited to be subjects in studies designed to assess and quantify the role of radiation exposure in the development of subsequent disease. More than 100 epidemiological studies of medically exposed populations have provided quantitative information on cancer risk (*1*), with data that can be generalized for comparison with risk estimates from other studies (*2*, *3*).

Medical studies offer special advantages. Exposures are given under controlled conditions that are generally well documented, and comparison subjects are readily available. The range of doses allows dose–response evaluations. They provide information on effects from high doses, which would be fatal if given as whole-body doses. These studies also provide information on interaction of radiation with other environmental factors, such as smoking and chemotherapy, and interaction with genetic susceptibility. Radiation-induced tumors do not differ from other tumors; therefore, they can provide insight into the carcinogenic process.

Epidemiological studies require dosimetry methods that estimate organ doses inside and outside radiation beams. The accurate estimation of absorbed dose to specific organs and tissues for individual study subjects permits quantification of risk as well as assessment of dose–response relationships and the modifying effects of age, sex and other treatments. Radiation therapy typically involves the delivery of high doses to the treatment site; absorbed dose to other organs varies and depends largely on the distance from the treatment site.

Radiation doses for epidemiological studies can be reconstructed many years after exposure, even without benefit of complete exposure information. Computing the dose to organs outside the treated volume is particularly challenging because dose decreases rapidly with distance, and uncertainty about the precise location of the treatment area translates to uncertainty in the dose at the point of interest. Even within a single organ, the dose may vary considerably.

The purpose of this review is to describe how we estimate the absorbed dose from external-beam radiation therapy, brachytherapy and diagnostic radiology and to provide case study examples of doses used in epidemiological studies. Methods of assessing the dose from internal radionuclides are well documented elsewhere and are not discussed here (*4*).

[1] Address for correspondence: The University of Texas M. D. Anderson Cancer Center, Department of Radiation Physics, Unit 544, 1515 Holcombe Blvd., Houston, TX 77030; e-mail: mstovall@mdanderson.org.

MATERIALS AND METHODS

Collection and Management of Patient Data

Because dose estimates are based on each patient's individual treatment parameters, the quality of retrospective data depends on how complete and accurate the treatment records are for each subject. Diligence is required to obtain details documenting all radiation therapy prior to the diagnosis of the health outcome under investigation. For external-beam radiation therapy, the records should include radiation energy, field size, anatomic location of fields (diagrams or photographs), treatment-planning details, daily treatment logs, and any other information relevant for reconstructing treatments. For brachytherapy, the record should include the radioactive isotope used, the activity of sources, duration of treatment, and anatomic location of the implant. For certain complex studies, such as studies of lung or breast tumors after treatment for Hodgkin lymphoma, additional documentation, including simulator films, photographs of the patient in the treatment position, and information describing the specific location of the second tumor should be obtained.

Our studies show that with sufficient effort, complete radiation therapy records can be obtained for approximately 85–90% of patients, depending on the primary disease site, calendar year, and treatment institution. Records are abstracted and coded by trained personnel, and at least 10% of the records are independently coded again by a dosimetrist or another abstractor. A higher percentage of the more complex records are reviewed for quality control. Data from the abstracted records are input electronically, and edit checks are performed to identify outliers and inconsistencies in the data. When a parameter is unknown, some values can be imputed for dose calculations by using other subjects' data from the same institution, same period, or both.

Documentation of studies of radiation exposures resulting from diagnostic testing typically includes only a written description of the type of examination, with no details of the machine parameters. Sometimes information on procedures can be obtained from current staff or institutional archives in the diagnostic radiology department. In the absence of specific machine parameters, organ dose is estimated on the basis of typical values reported in the literature for a given examination and time.

Estimation of Radiation Absorbed Dose to Organs

1. External-beam radiation therapy

The three major components of absorbed dose outside treatment beams from external-beam radiation therapy are: (1) radiation leakage through the head of the machine, (2) scatter off the beam collimators, and (3) scatter within the patient from the primary beam. To estimate organ doses from these sources for an epidemiological study, three techniques are used: (1) calculation using a three-dimensional (3D) mathematical computer model based on measurements made in a water or polystyrene phantom, (2) direct measurement in an anthropomorphic phantom constructed of tissue-equivalent material, and (3) calculation of dose using a treatment-planning computer.

a. 3D mathematical computer model

With this system, absorbed dose outside the treatment beam is measured on a 3D grid in a large water or polystyrene phantom. The radiation detectors used are thermoluminescence dosimeters (TLDs) containing lithium fluoride or calcium fluoride powder in capsules or chips. The response of the TLD is standardized in a ^{60}Co beam with output measured by the Accredited Dosimetry Calibration Laboratory at M. D. Anderson Cancer Center, which is approved by the National Institute of Standards and Technology. TLD measurements are verified independently by ionization-chamber measurements at selected points.

Figure 1 shows a beam's-eye and lateral view of the out-of-beam measurement setup (*5*). Dosimeters are placed in a phantom on a 3D grid at various depths from the surface and at distances out to 70 cm perpendicular to the central axis. Dosimeter spacing depends on radiation energy. Data are typically measured for field sizes of 5 × 5, 10 × 10, 15 × 15, and 20 × 20 cm^2. We have an extensive library of measured out-of-beam data, including orthovoltage X rays (1 to 3 mm copper half-value layer), ^{60}Co γ rays, and high-energy photons (4–25 MV). Figure 2 shows examples of out-of-beam data measured in water for 10 × 10-cm^2 beams of six photon energies at a depth of 10 cm (*5–7*).

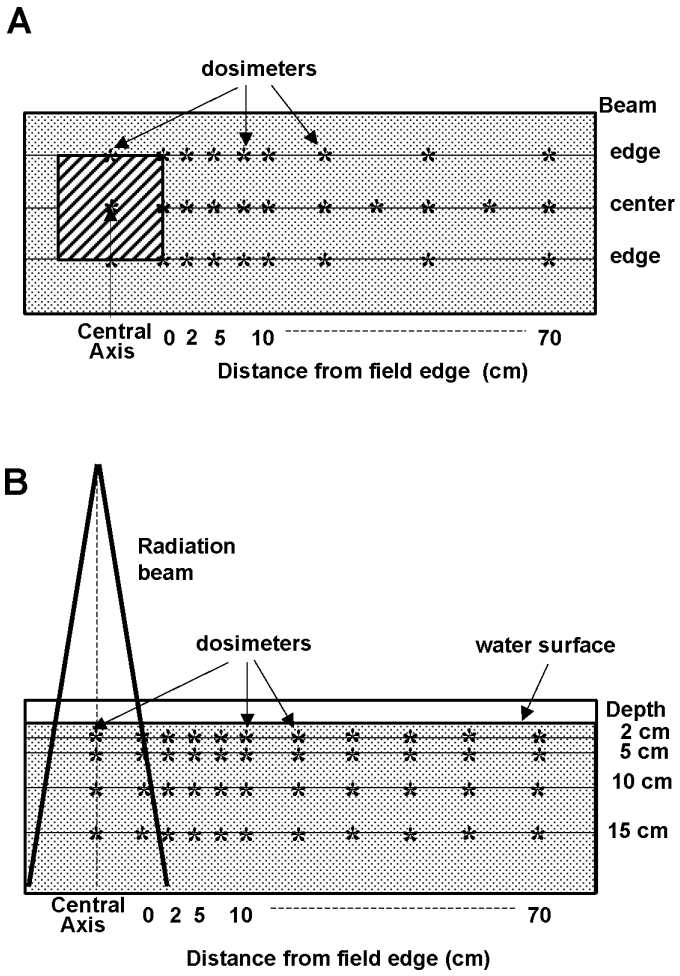

FIG. 1. Water phantom setup for out-of-beam measurements. Panel A: Beam's-eye view. Panel B: Lateral view. Reprinted from ref. (*5*) with permission from Elsevier.

The dose from a beam is divided into three regions for calculation of dose at any point. ''In-beam'' dose is calculated using depth–dose data in clinical use (*8*). ''Near-beam'' dose is calculated using a log-linear interpolation between points of measurement; this region varies from 7–15 cm from the beam's edge, depending on radiation energy. ''Far-outside-beam'' is calculated using a curve derived from measured data. For field sizes other than those measured, a linear interpolation between doses for measured field sizes is used.

A three-dimensional mathematical computer model of the human body was designed to describe the external dimensions of a patient using a set of regular, geometric shapes (right-angle parallelepipeds) that can be described by simple mathematical expressions. Our mathematical computer model can be used to simulate a person of any age, based on body-size measurements made for a National Safety Council (NSC) study conducted by the Society of Automotive Engineers (*9*). NSC measurements were made in 1972 on more than 4,000 children from the United States

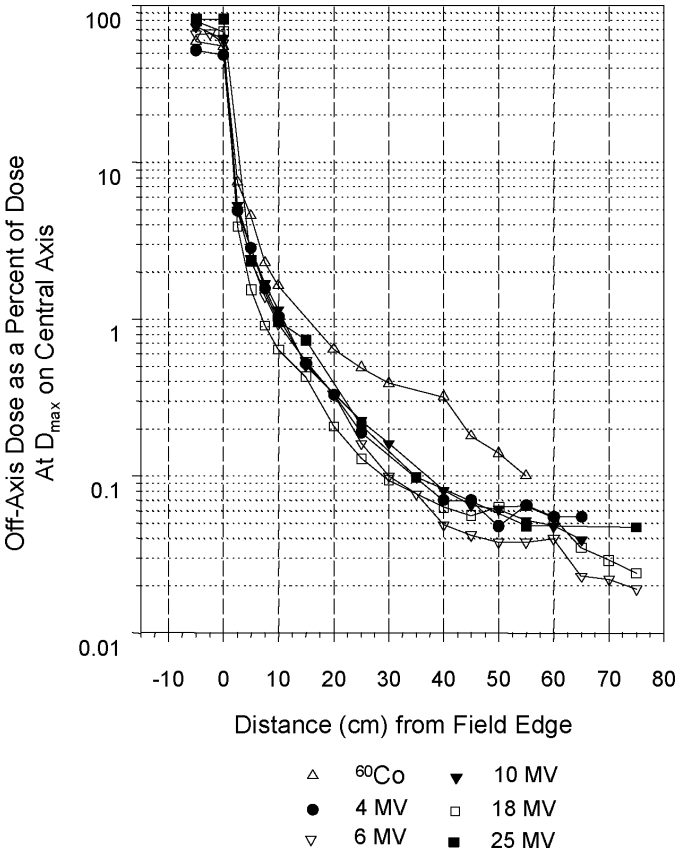

FIG. 2. Total absorbed dose in a water phantom from 10 × 10-cm^2 fields of ^{60}Co γ rays and 4, 6, 10, 18 and 25 MV photons at 10 cm depth, normalized to 100% on the central axis at depth of maximum dose. Reprinted from ref. (*5*) with permission from Elsevier and from refs. (*2*) and (*3*) with permission from *Medical Physics.*

who were between the ages of 3 months and 19 years. Our mathematical computer model was designed specifically for seven age groups: newborn and patients 1, 3, 5, 10, 15 and 19 (adult) years of age, with sizes of patients between these ages calculated by linear interpolation. The age-specific sizes of children for individual patients or populations of patients may not correspond to data from the 1970s in the United States; in this case, the phantom size can be selected by specifying height.

Figure 3 shows a frontal view of the 1-, 3-, 5-, 10- and 15-year-old phantoms and the adult phantom (*5*). The arms and legs of the phantoms can be moved to simulate the patient's position during treatment. The overall height of the phantom, relative to age, was compared to growth charts[2] supplied by the Centers for Disease Control, with good agreement. The same heights are used for males and females. Figure 4 shows that the average height for both sexes is essentially the same before age 15 years (*5*).

The phantom is divided into five sections: head, neck, trunk, arms and legs. Using several atlases of anatomy (*10–14*), the locations of 29 organs are specified within the phantom: the brain, pituitary gland, parotid glands, sublingual glands, submaxillary glands, larynx, thyroid, breasts, heart, lungs, adrenal glands, kidneys, stomach, gallbladder, pancreas, liver, small intestine, ascending colon, transverse colon, splenic flexure, descending colon, sigmoid, rectum, bladder, prostate, testes, ovaries, uterus and vagina. The organs are represented by 1,400 individual points; these points are evenly spaced within organs to allow calculation of minimum, maximum and average doses. Additional organs or calculation points are added as needed. The locations of bone and active bone marrow (ABM) are also specified within the phantom and are divided into partitions; the proportional weight of each partition depends on the patient's age (*15, 16*).

To calculate the dose to an anatomic site for a particular type of treatment, the beams are positioned on the mathematical computer model, with beam size, radiation energy, and treatment dose specified. Plane geometry is used to calculate the lateral distance from the nearest field edge and the depth from the surface to each of the points in the organs

[2] Center for Disease Control, Standard Growth Charts, www.cdc.gov/nchs/about/major/nhanes/growthcharts/clinical_charts.htm, 2002.

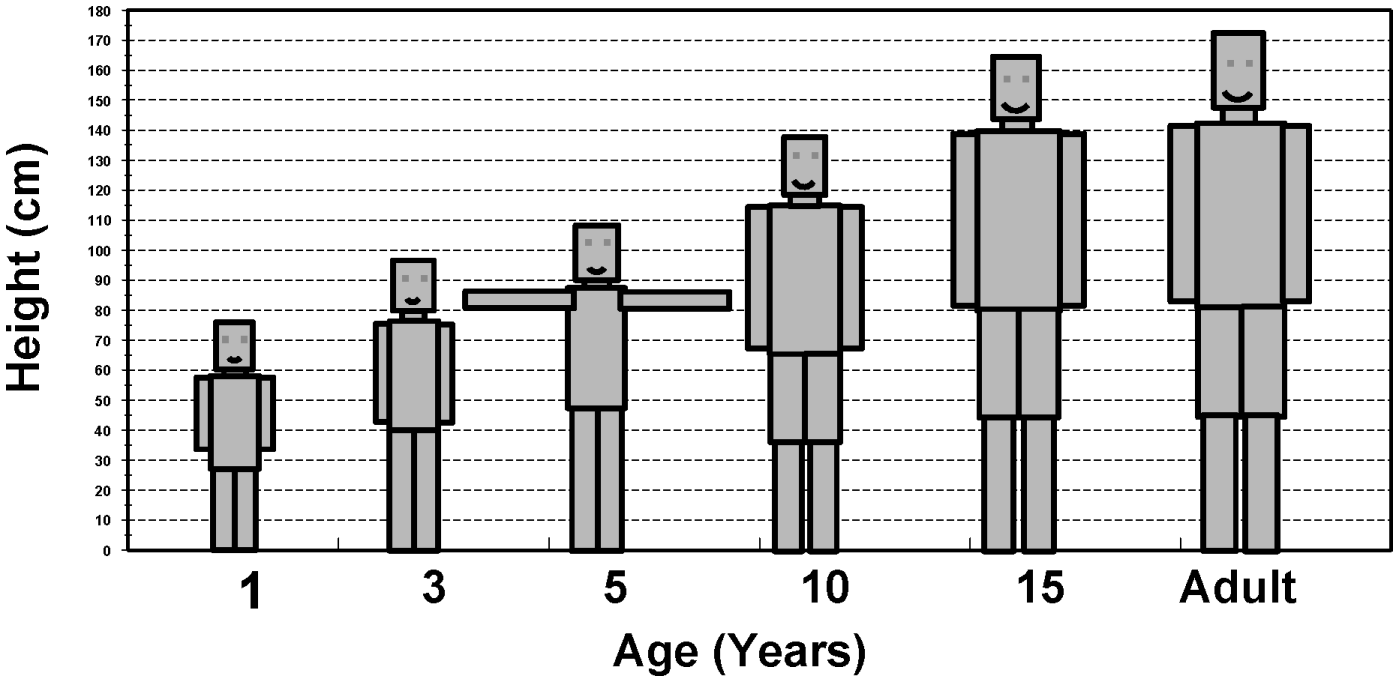

FIG. 3. Mathematical computer model, ages 1 through 15 years and adult. Reprinted from ref. (*5*) with permission from Elsevier.

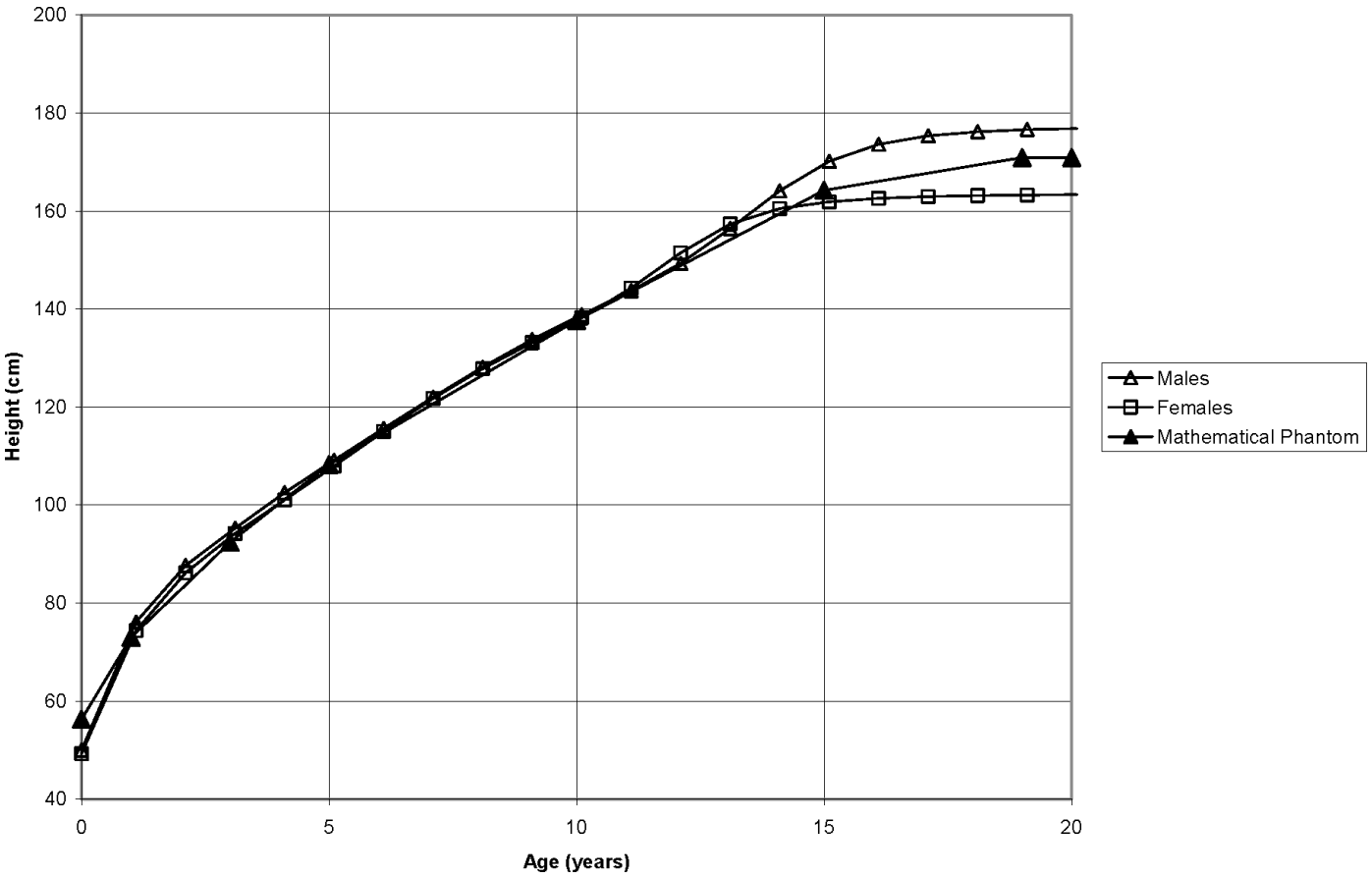

FIG. 4. Average height by sex[2] and mathematical computer model height. From ref. (*5*) with permission from Elsevier.

or anatomic regions of interest. This calculation method is suitable for estimating dose at any distance from beams.

b. Anthropomorphic phantom

Doses to organs can be measured directly in an anthropomorphic phantom. Three sizes of commercially available Alderson Rando[3] phantoms are used: adult male, adult female and 6-year-old child (Fig. 5). The phantoms can be modified for specific patient characteristics, such as various breast sizes. The phantoms are constructed of three densities of tissue-equivalent material that closely simulate the composition of the human body (e.g. soft tissue, lung and bone). Dosimeters are placed throughout the phantom on a 1.5-cm grid at locations determined by the requirements of the particular study. The phantom is irradiated using the same techniques used to treat a patient (Fig. 6). Typical irradiation requires several hundred dosimeters for a 3D mapping of a region of interest.

c. 3D treatment-planning computer

The method of choice for calculating dose to anatomic regions in or near the radiation beam used for cancer therapy is a commercially available treatment-planning system, such as the ADAC Pinnacle[3] System (Philips Radiation Oncology Systems, Milpitas, CA). Such a system is suitable for irregularly shaped beams with special blocking, such as mantle fields or inverted-Y fields (Fig. 7), which are used to treat patients with Hodgkin lymphoma. This method is limited to estimating doses to organs that are close to the anatomic site being irradiated. However, in most epidemiological studies, doses to distant organs are required and this method would not be applicable.

d. Comparison of the methods to reconstruct doses from external-beam radiation therapy

Each of the techniques used for estimating the radiation dose absorbed by organs outside the treatment site during therapy has advantages and disadvantages. An anthropomorphic phantom is the closest simulation of the irradiation of a patient; however, absorbed-dose measurements obtained using this system are valid only for specific irradiation conditions, are expensive, and are limited to phantoms of only a few sizes. The 3D mathematical model is much less expensive to use, can simulate a patient of any age or size, and offers complete flexibility in the selection and placement of treatment beams. The treatment-planning system is suitable only for situations requiring precise estimation in or near beams. In general, anthropomorphic phantoms are used for studies of adults receiving highly standardized treatments, with a limited range of field sizes, locations and beam energies. The mathematical model is most suitable when there is large variation in patient size, such as in a pediatric population, or when a study includes a variety of radiation therapy techniques or many anatomic regions of interest. To ensure consistency, we verify that the results agree where two or more methods are applicable.

2. Brachytherapy

Brachytherapy is ''short-distance'' therapy in which radiation is delivered through tubes, needles or seeds placed in or on the patient. For

[3] Alderson Radiation Therapy Phantoms, www.pi-medical.nl/rs/rs-art.htm, 2002.

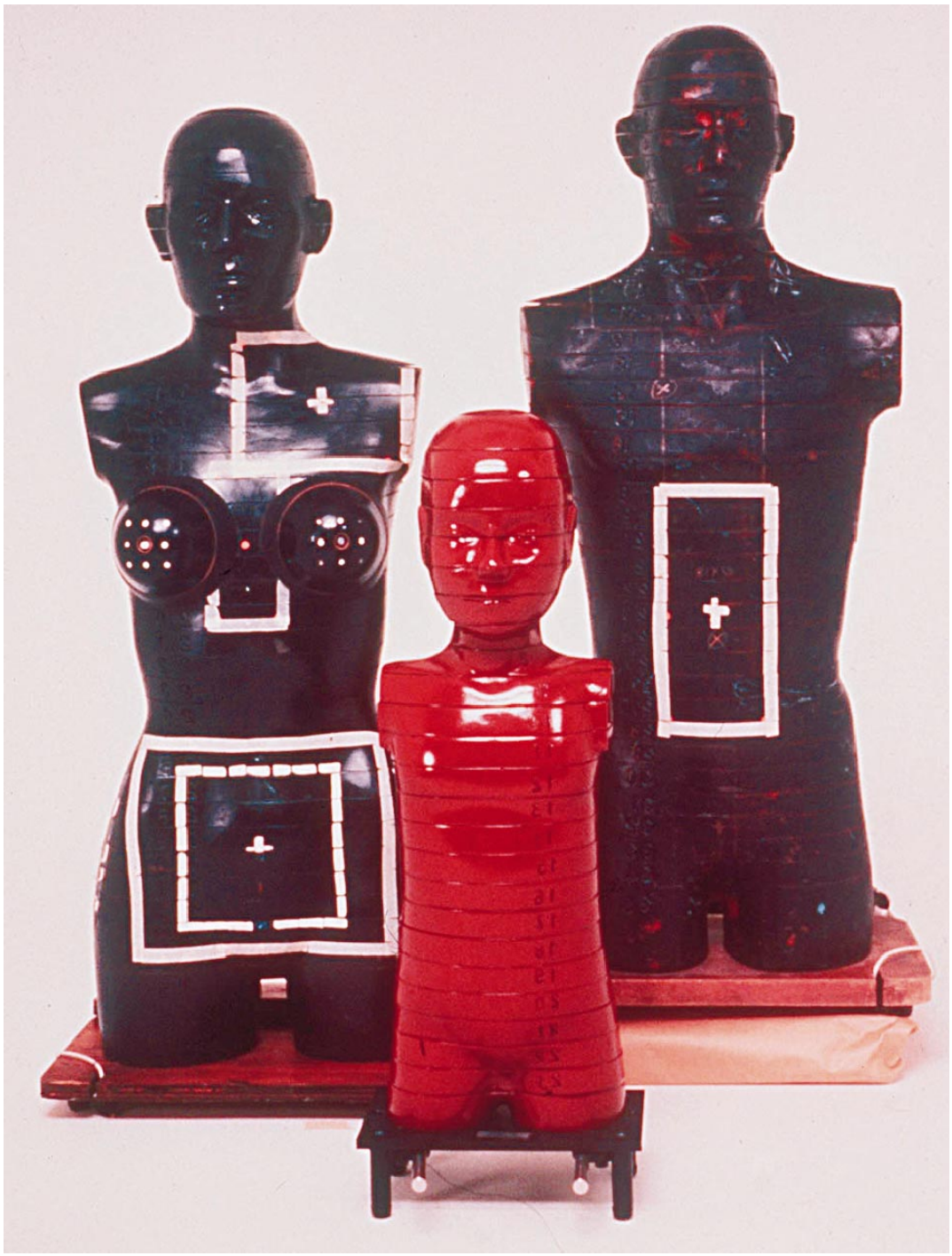

FIG. 5. Anthropomorphic (Alderson-Rando) phantoms, adult male, adult female, and 6-year-old child.

clinical use, dose from sealed brachytherapy sources is calculated using isodose curves to estimate prescribed doses. This method is applicable to sealed sources of ^{226}Ra, ^{60}Co, ^{132}Cs, ^{198}Au, ^{125}I or ^{192}Ir (*17, 18*). For dose reconstruction, the mathematical computer model used for external-beam dosimetry, as described above, is used to calculate the distance from a radioactive source to the sites of interest. The validity of this method for estimating dose at distances far from the source has been verified by measurements in an Alderson-Rando phantom (*19*).

3. Diagnostic X-ray examinations

Ideally, one can calculate dose from a diagnostic examination using software based on Monte Carlo simulations that take into account particular machine parameters, such as kVp, filtration, field size and skin entrance exposure. However, because machine parameters are rarely available in medical records, we must use typical data for the examination and period of interest. This is a two-step process: describing the exami-

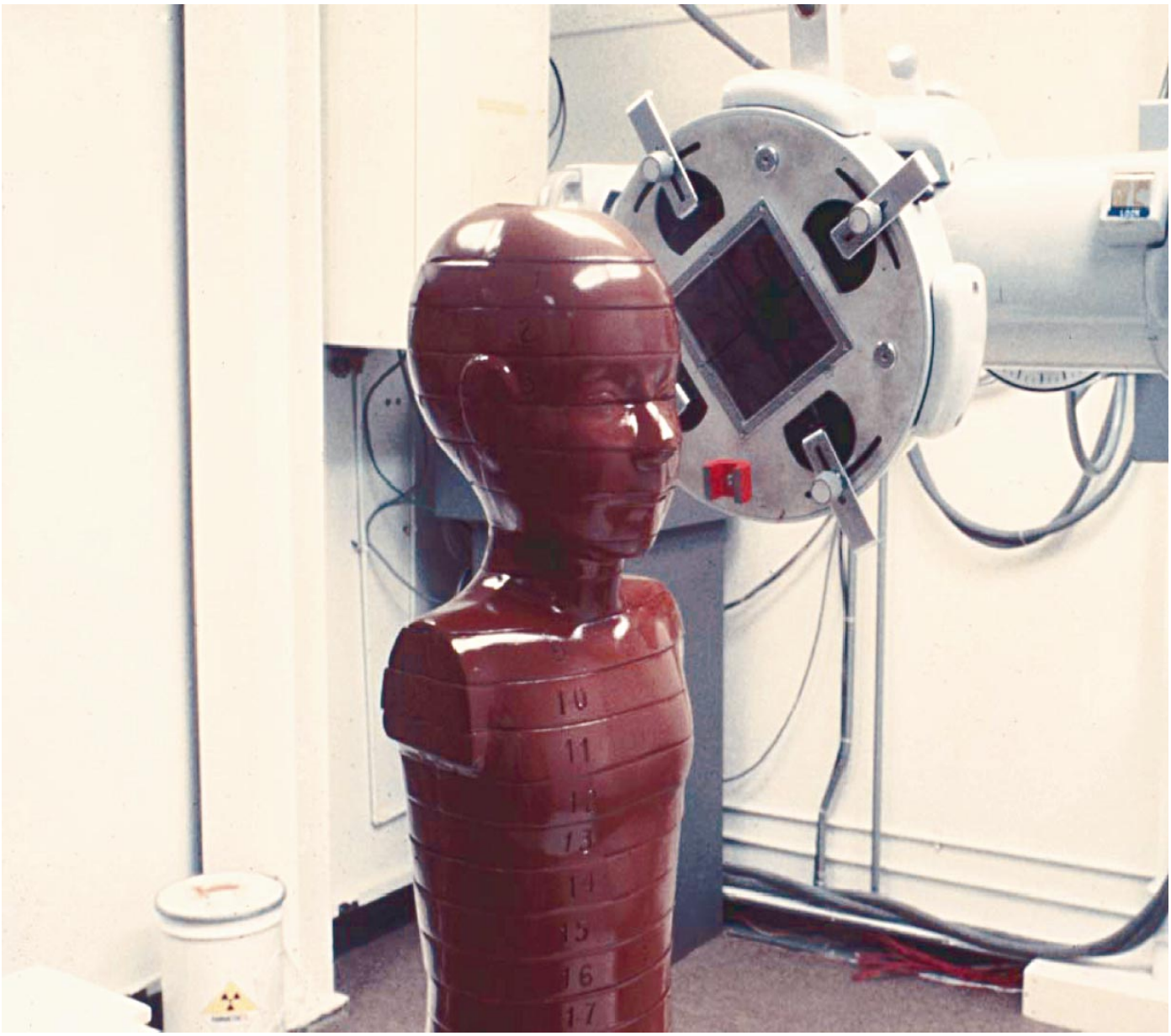

FIG. 6. Anthropomorphic phantom (6-year-old child) positioned to simulate irradiation of the tonsil.

nation in terms of number and anatomic location of views (*20, 21*) and estimating dose from each examination. Data suitable for both steps have been published for various periods. Organ doses from diagnostic examinations can be calculated using published data (*22, 23*). It should be noted that organ doses from diagnostic examinations have changed dramatically over the past few decades. Doses have decreased substantially for many examinations due to improved technology; at the same time, however, the use of new high-dose examinations, such as CT scans, has increased. In an epidemiological study, it is essential to use dose estimates for the appropriate period.

Doses from diagnostic procedures are subject to greater uncertainty than those from therapeutic exposures. Patient records of diagnostic examinations are likely to be limited to the type of procedure performed and the clinical findings; it is unlikely that documentation of machine parameters will have been included. Furthermore, repeat exposures to improve image quality are common, yet these would not be included in the documentation. For fluoroscopic examinations, the machine ''on time'' is highly variable but is not included in the documentation. Also, older machines in operating condition are rarely available for use in performing measurements. For plain-film radiography, it may be necessary to use machine parameters such as kVp, filter and field (film) size from a few representative records containing this information and to interview staff who are familiar with the institution's older equipment and procedures. Uncertainties for diagnostic exposures are more likely to underestimate the dose, resulting in risk estimates biased on the high side.

For all studies, quality scores are assigned to each individual's dose estimates. These scores reflect the type and completeness of documentation received and other factors that might introduce uncertainty in the dose estimates.

RESULTS

Using the methods described above, organ doses have been estimated for numerous epidemiological studies (see

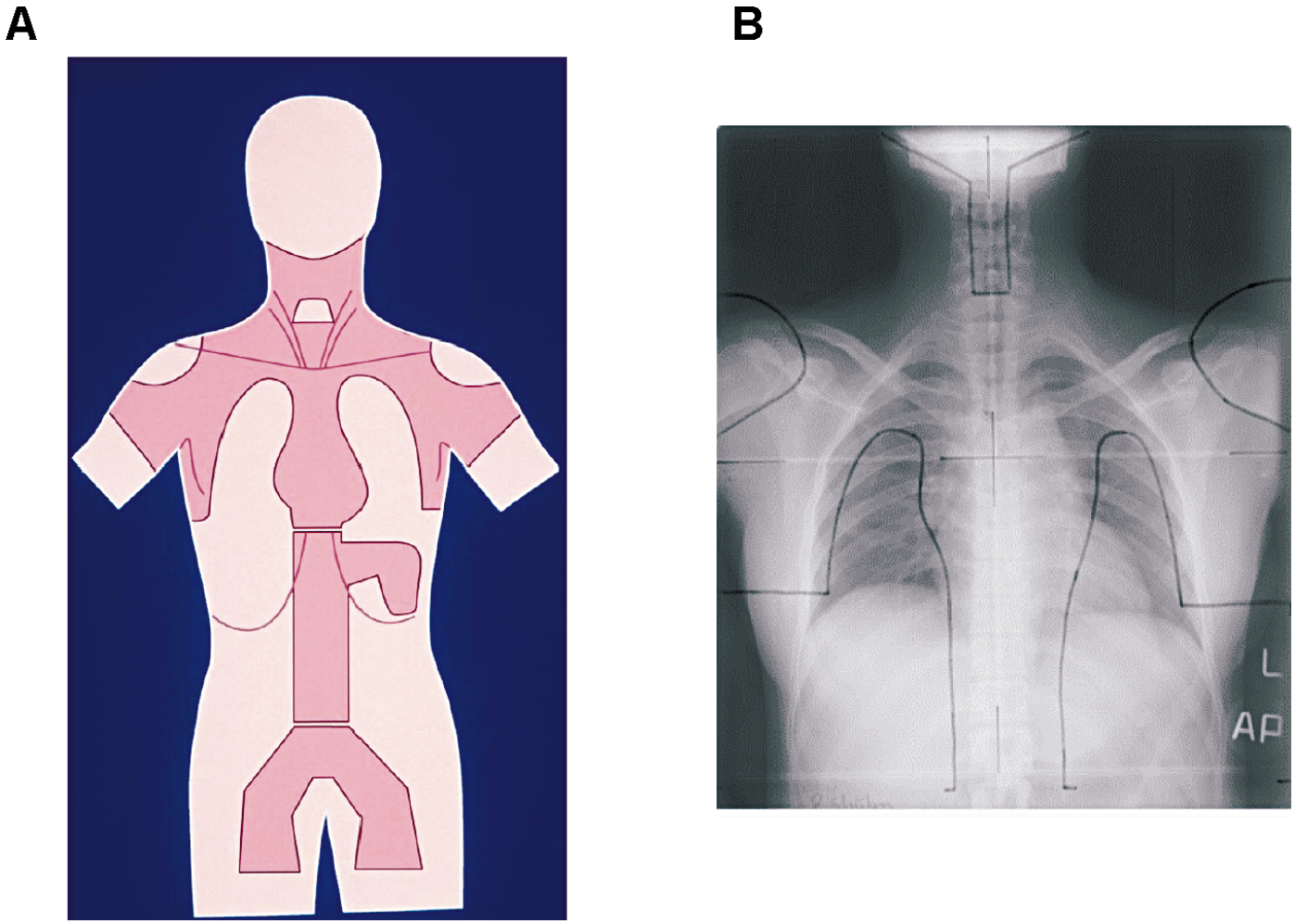

FIG. 7. Typical blocked fields used to treat Hodgkin lymphoma. Panel A: Diagram. Panel B: Simulator radiograph of a mantle treatment.

Table A1 in the Appendix). Discussions of selected studies illustrate special applications and examples of dosimetry methods.

Radiation Therapy for Tinea Capitis in Childhood

From the 1930s through the 1950s, in many countries children were treated with external-beam radiation therapy for tinea capitis (ringworm of the scalp). Epidemiological studies were conducted of populations treated in Israel (*24, 25*) and New York City (*26–28*); these are important because they provide estimates of risk at relatively low doses. Special headgear was used to position five fields on the scalp using the Adamson-Kienbock technique (*29*). Three independent retrospective dosimetry experiments were conducted by other investigators using original treatment X-ray machines and headgear to irradiate an anthropomorphic phantom (*24, 27, 30*). In each experiment, assumptions were made about the following patient data: shape and size of the head, thickness of the skull, and patient position during treatment. For the study conducted in Israel (see item 2.7 in Table A1), we used the measurements of Schulz and Albert (*27*) to estimate age-specific radiation doses to the brain and scalp (*31*) and to the thyroid (*32*). Although individual treatment plans were not available, highly standardized, well-documented treatments were given in three clinics; these data were adequate to estimate doses for patients treated at those clinics. However, due to the uncertainties in the individual dose estimates, a comprehensive evaluation of uncertainties in dosimetry was undertaken, with respect to radiation-induced risks for thyroid tumors. The uncertainties in each element of the dosimetry procedure, such as machine calibration, beam quality, patient positioning, and movement of patients during treatment, were assessed. When the data were reanalyzed, taking these dosimetric uncertainties into account, they appeared to have only a minimal effect on the risk estimates (*33, 34*).

Tonsil Irradiation during Childhood and Adolescence

Approximately 4,000 patients treated during childhood with external-beam radiation therapy for lymphoid hyperplasia of the tonsils were evaluated retrospectively to determine whether the treatment was associated with subse-

quent development of malignant or benign thyroid nodules, salivary gland tumors, and hyperparathyroidism (*35–37*). Although the original treatment machine was no longer available, dose measurements were made using a similar but more modern machine with dosimeters placed in an anthropomorphic phantom representing a 6-year-old child (Fig. 6). Approximately 70% of the children had been treated with rectangular fields and the other 30% had been treated with square fields; the records were unclear about orientations of the rectangular fields. Therefore, doses were estimated in three ways: long-dimension vertical, short-dimension vertical, and an average of these two dose estimates. Risk estimates based on an average of the two rectangular fields were similar to estimates based on doses for the 30% of patients treated with square fields (*35*).

Radiation Therapy for Peptic Ulcer

A cohort of 3609 patients treated by external-beam radiation therapy for peptic ulcer from 1937 through 1965 was evaluated retrospectively for development of subsequent malignancies and heart disease (*38–40*). Our measurements were made in a male Alderson-Rando phantom using the original treatment machine, which had a special lead rubber shield to reduce the dose to organs adjacent to the stomach. In addition, staff members who treated some of the patients were able to verify phantom setup and provide details of treatment that had not been recorded in the treatment records. The use of the original equipment and participation of treating staff resulted in high-quality dosimetry estimates for evaluation of malignancies. The estimation of cardiac doses, however, was not straightforward, because approximately 5% of the heart was estimated to be in the radiation field and received both scatter and direct radiation, whereas the remainder of the heart received only scatter radiation. The determination of the percentage of the heart in the beam was based on fluoroscopic examination of each patient to verify the location of the beam and adjacent organs. Measurements were normalized to each patient's prescribed stomach dose, which was obtained from the individual radiation therapy records, to obtain the volume-weighted mean dose to each patient's heart. The total average cumulative cardiac dose for each patient was obtained by summing the volume-average cardiac dose over all treatment courses.

Lung Cancer after Radiation Therapy for Hodgkin Lymphoma

We evaluated doses to various lung sites for a study of the risk of lung cancer after treatment for Hodgkin lymphoma (*41, 42*). This was the first epidemiological study of radiation-induced lung cancer after Hodgkin lymphoma to take into account the dose received at the specific site of the subsequent tumor in the lung. Studies of subsequent cancers in patients with Hodgkin lymphoma can be difficult due to irregularly shaped treatment fields; Fig. 7 shows that the lungs are partially blocked during such treatment. Because blocking attenuates the dose to approximately 10% of that from the primary beam, it was important to know the site of the lung tumor relative to the blocking. Two types of information were required for dosimetry: (1) location of the chest fields using simulator films and radiation records and (2) location of the lung tumors using diagnostic pathology reports, surgical/bronchoscopy notes, hospital records, and radiological studies, including copies of chest X rays, CT scans, and tomograms. For each case/control set, a radiation oncologist reviewed all the information and determined the location of the secondary lung cancer in the case relative to the radiation fields in the case and matched controls (*41, 42*). Because of the large range of dose to the lungs, it was essential to determine dose to the specific site of the lung tumor; mean dose throughout the lungs would have been inappropriate.

Sarcomas after Radiation Therapy for Retinoblastoma

Hereditary retinoblastoma is a rare tumor of the eye that usually occurs in children under 2 years old. Survivors are at high risk of developing a subsequent sarcoma of the bones or soft tissue (*43*). Patients in our study were irradiated by external-beam radiation therapy (90%), brachytherapy (1%), or a combination of these techniques (9%). The common external-beam treatments in this cohort were a two-field technique with nasal and lateral fields and a single-field technique with either a lateral or anterior field. Before 1960, orthovoltage X rays were the most common type of external-beam radiation used; after 1960, 22–23 MV photons became the most widely used form of external-beam radiation. In our study group, tumor doses to the affected eye ranged from 15–115 Gy (average, 48 Gy), with the highest doses delivered from orthovoltage machines. Brachytherapy treatments were delivered by means of eye plaques, which contained radon seeds prior to 1960 and ^{60}Co in later years.

Patients were treated with machines fitted with special cones to define the small eye fields. Because many of the sites of interest were near the treated eye in a region of rapid fall-off, out-of-beam measurements of the dose distribution near the cones were made with TLDs and film. The mathematical computer model was used for dosimetry estimates; Fig. 8 shows doses for a typical external-beam treatment of a 2-year-old child. The tumors were located as precisely as possible, based on clinical notes, pathology reports, and radiology reports. When there were uncertainties about the location of subsequent tumors, the average of the minimum and maximum estimated doses for sites of interest was used.

Second Cancers after Radiation Therapy for Cancer of the Uterine Cervix

We provided dosimetry for case/control studies of second tumors for patients drawn from a large international cohort

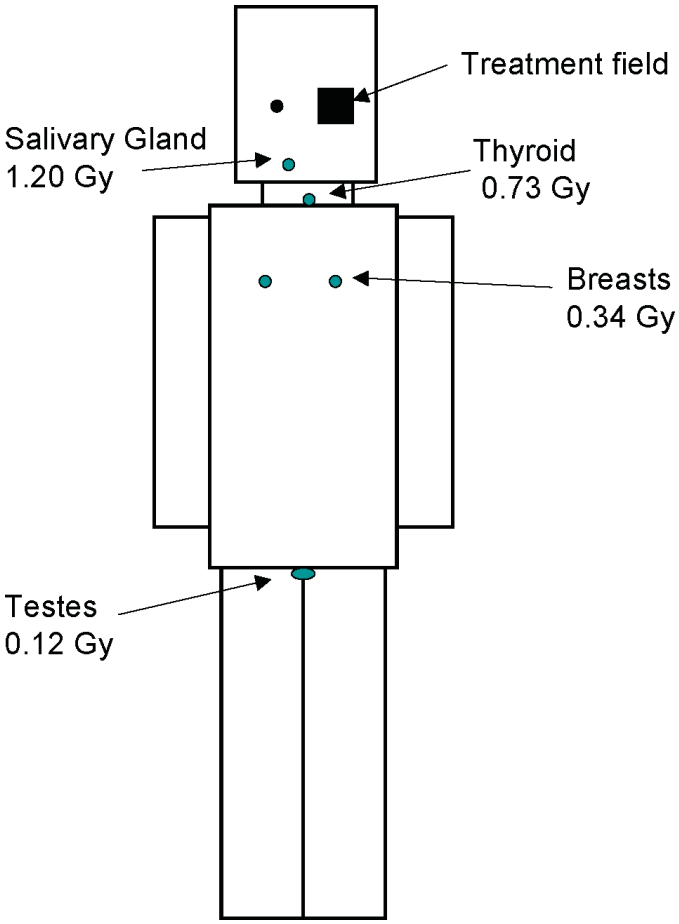

FIG. 8. Mathematical computer model; doses to selected organs of a 2-year-old patient with retinoblastoma treated to 45 Gy with a ^{60}Co γ-ray beam.

(*44*). The radiation therapy was highly standardized according to stage of cancer, with the majority of patients receiving both external-beam and brachytherapy (*19, 44–46*). We estimated dose in three ways: (1) measurement of the dose in an Alderson-Rando phantom, (2) calculation of dose using the computer model described above, and (3) calculation of internal scatter dose from the primary beam using a Monte Carlo calculation. To make the Monte Carlo calculation comparable to the total-dose measurements, we added the contribution from the other components (i.e., head leakage and collimator scatter). Dosimetry values selected for the analysis were derived from all three sets of data (*19*).

For the study of subsequent leukemia, the ABM dose was calculated as a weighted average to the ABM using the partitions and weights reported by Cristy (*16*). The dose to the ABM partitions ranged from 0.001–5.5 Gy (*45*), which allowed investigators to model the risk of leukemia, taking into account doses that could potentially cause cell killing rather than cell mutation.

To validate doses, we conducted an extensive comparison of organ doses estimated by calculation using the mathematical computer model and by measurements using TLDs in an Alderson-Rando phantom (*19*). The anthropomorphic phantom irradiations used the same TLD system that was used for the water phantom measurements. Table 1 lists results of the two methods to estimate dose from anterior and posterior pelvic fields. The methods differ because for each organ there are many more points of calculation in the mathematical computer model than points of measurement in the anthropomorphic phantom. Estimates of mean dose to the ovaries, which are in the primary beam, agreed within ±7% using both methods. Overall agreement between these two methods was within 20% for most organs, with only the dose to the thyroid gland showing greater discrepancy. This agreement is acceptable from the perspective of the large range of doses outside a beam, where dose can decrease significantly near the edge of the beam.

Diagnostic Radiation for Scoliosis

In a study of 5573 adolescent girls who had frequent radiographic examinations of the spine as part of the man-

TABLE 1
Comparison of Absorbed Doses of Radiation (Gy) Estimated Using a Mathematical Computer Model and an Anthropomorphic Phantom AP/PA[a] Pelvic Fields[b]

Organ	Mathematical computer model (average of many points for each organ)	Anthropomorphic phantom Alderson female (average of TLDs in several phantom slices)
Brain	0.05	0.06
Breast	0.29	0.30
Kidney	1.40	1.30
Lung	0.26	0.30
Ovaries	36.70	34.40
Salivary glands	0.07	0.10
Stomach	0.87	0.89
Thyroid	0.10	0.14
Total active bone marrow	8.18	8.31

[a] AP, antero-posterior; PA, postero-anterior.
[b] ^{60}Co γ rays, 15-cm × 15-cm^2 field size, 80-cm source-skin distance, and 30-Gy dose to D_{max} each field.

agement of scoliosis, we estimated the doses to the breasts associated with the radiation exposures (*47*). Based on the number of examinations performed, the calendar years of examinations, and the patient's age, the breast dose was estimated at a 1.0-cm depth for pre-teens and a 2.5-cm depth for teens, using a software package[4] based on organ doses calculated by Rosenstein (*22*). The examinations spanned several decades and breast doses varied over that period. Medical records documenting the diagnostic examinations of the spine, including machine parameters, were available for only about 25% of the patients. However, because these examinations were standardized, it was possible to make assumptions about irradiation conditions for patients with missing data and to estimate a breast dose for each study subject. The average estimated cumulative breast dose was 0.11 Gy (range, 0–1.70 Gy).

DISCUSSION

Epidemiological studies of medically irradiated populations contribute an important body of evidence to what is already known about risks for radiation-induced cancers. These studies have significantly increased the capability to reconstruct doses to individual organs that allows detailed dose–response analyses and increases their use as prediction mechanisms (*3*).

Several methods used to estimate organ doses during radiation treatment or diagnostic examinations have been described in this paper; each method has advantages and disadvantages. Despite the unlimited number of points of calculation in the mathematical computer model and the availability of all ages, the advantage of the anthropomorphic phantoms is that, because of their human-like contours and densities, they more realistically simulate the scatter and absorption of radiation in patients. If the treatment under study was mainly administered to adults, with a limited range of field sizes, locations and beam energies, the anthropomorphic phantoms offer an advantage of enhanced realism. Their disadvantages are that they are available only in a limited number of sizes, irradiation is expensive and time consuming, and results of an irradiation are applicable to only one specific set of treatment parameters. In addition, the fixed grid of holes to hold dosimeters allow for only a limited number of measurement points. The advantage of the mathematical computer model is that it allows flexibility in patient size, organ locations, number of points of calculation, and beam orientation.

The aim of radiation therapy is to deliver a radiation dose adequate to kill tumor tissue but spare healthy tissue (*48*). An array of sophisticated imaging and treatment-planning systems is available to achieve that aim with high precision. Realistically, however, that same level of precision cannot be achieved in epidemiological studies that are aimed at retrospectively estimating individual organ doses for a large number of patients.

There are two primary sources of uncertainty in dose estimates: (1) Patient information, which includes details abstracted from the patient's record as well as information provided by the institution about equipment and usual treatment techniques. This is the largest source of uncertainty and determines the quality of dosimetry data. (2) Methods selected for dose estimation, which include measurements in an anthropomorphic phantom, water phantom measurements applied to a mathematical computer model, Monte Carlo calculations, or a combination of these methods.

Uncertainties in dosimetry can include misspecification of tumor position with respect to the treatment fields; missing information on the use of shielding, field sizes and orientation, and blocking position; and incorrect recording of treatment doses. In most epidemiological studies that estimate the risk of late effects due to radiation treatment, it is unlikely that there will be any systematic bias in the estimation of dose that could distort the estimation of risk; however, there will be random variation associated with any exposure misclassification. In any study, one should aim to be consistent across a population of patients and produce dose estimates that do not differ systematically between cases and a comparison group. Selection of the best method of dose estimation or best combination of methods involves consideration of the study population, sites of interest, and treatment regimens. Despite unavoidable sources of uncertainty, it is possible to estimate radiation doses to organs outside the treatment field that can be used in epidemiological studies. In fact, the analysis by Lubin *et al.* (*34*) showed that relatively large uncertainties in dose estimates for patients treated for tinea capitis did not have a serious impact on risk estimates. However, the studies of breast and lung tumors after Hodgkin lymphoma required special effort to determine dose to the specific site of the second tumor; this effort was necessary because patients were treated with irregularly shaped blocked fields, which produced doses within the breast and lung that varied by a factor of ten (*41, 49*).

Details concerning a subject's size at time of treatment and the location of internal organs are not usually available many years after treatment delivery. Frequently, the organ of interest with regard to late effects was not imaged or located at the time of treatment. This situation can be problematic, because retrospective dosimetry estimates must then be based on average organ sizes and locations. Uncertainties and errors in placement of field(s) during the original treatment and location of the organ of interest relative to the treatment field are particularly critical to retrospective dose estimation when the organ is close to a field edge (<5 cm) because of the rapid fall-off of dose next to the edge of the treatment field (Fig. 2).

[4] XRAYDOSE, MHP Software, North Little Rock, AR.

TABLE 2
Additional Dosimetry Methods for Epidemiological Studies

Condition/site treated	Method of dosimetry	Reference(s)
Tuberculosis (fluoroscopies)	Anthropomorphic phantom and Monte Carlo calculation	Boice *et al.* (*58*)
Ankylosing spondylitis	Anthropomorphic phantom	Court-Brown *et al.* (*59*)
Pediatric cancer	Software developed for retrospective studies	de Vathaire *et al.* (*60, 61*)
Tinea capitis	Anthropomorphic phantom	Harley *et al.* (*62*)
Thymus	Mathematical phantom and Monte Carlo calculation	Hildreth *et al.* (*63*)
Benign locomotor	Anthropomorphic phantom	Johansson *et al.* (*64*)
Ankylosing spondylitis	Mathematical phantom and Monte Carlo calculation	Lewis *et al.* (*65*)
Hemangioma	Anthropomorphic phantom	Lundell (*66*)
Benign breast disease	Anthropomorphic phantom	Mattsson *et al.* (*67*)
Tinea capitis	Anthropomorphic phantom	Schulz and Albert (*68*)
Ankylosing spondylitis	Monte Carlo calculation	Weiss *et al.* (*69*)

The relative contributions of the three components to total dose from external-beam treatments, i.e., scatter radiation within the patient, head leakage, and collimator scatter, have been reported by a few investigators. Fraass and van de Geijn (*50*) found that collimator scatter plus leakage is of the same order of magnitude as patient scatter. Kase *et al.* (*51*) also indicated that near the beam, the collimator scatter contributes 20–40% of the total peripheral dose and that leakage becomes the main contributor at greater distances from the field edge. Greene *et al.* (*52, 53*) found that collimator scatter was the dominant component of the peripheral dose near the treatment beam. Measurements indicate that, in general, machines of the same energy show the same proportion of dose due to scatter and head leakage and there is little error caused by using out-of-beam data measured on a single machine to represent other machines of the same energy.[5]

Van der Giessen (*54*) verified his calculation method using *in vivo* measurements on 147 adult patients during 490 treatment sessions. TLDs were placed on the perineum during treatment of a variety of tumors in the neck, thorax or pelvis, using radiation energies ranging from ^{60}Co to 25 MV photons. The ratios between calculated and measured ranged from 0.76 to 1.02, demonstrating that the calculation method was a practical method for estimating dose to sites of interest outside the primary treatment beam for the purpose of estimating risk.

Van der Giessen (*55*) also compared the basic data used in his peripheral dose calculation method with measurements reported in 16 publications, including data used in the method reported here, and found the overall agreement to be good. The largest discrepancies were at the highest photon energies. The standard deviation of the published values was reported to be 33% overall. Van der Giessen also investigated peripheral dose of elongated and irregularly shaped fields and found good agreement with peripheral dose for equivalent square fields.

François and colleagues (*56, 57*) described a mathematical computer model similar to ours, which is based on measurements in a water phantom. For individual organ doses, their data agree with our data to $\pm 30\%$, with no systematic differences. In a direct comparison between the phantom used by François and colleagues and our methods and phantoms, differences could be explained by differences in organ locations.

Other approaches have been used effectively and incorporated into epidemiological studies as listed in Table 2.

One area in which there is potential for future improvement in dose reconstruction is the characterization of sources of uncertainty, as well as total uncertainty, in individual estimated doses. How dosimetric uncertainties affect the shape and magnitude of the dose response is a concern within the epidemiological community (*70*). Characterization of uncertainty for medical irradiations is generally simpler than for occupational or environmental exposures because the exposures are controlled and there is documentation for most treatments or diagnostic examinations.

Dosimetry will continue to play an important role in the estimation of cancer risks after medical irradiation. With the introduction of new diagnostic and therapeutic techniques, additional cohorts of exposed patients are being identified, and individual organ dose estimates will be needed to adequately evaluate the long-term health effects associated with these new techniques. For example, in diagnostic imaging, a recent increase in the use of full-body CT scanning as an early-detection screening method for asymptomatic patients is of concern, especially if the patients are young children who undergo multiple screenings. The cumulative radiation doses from multiple CT scans may increase the risk of cancer in these patients (*71, 72*). In therapy, intensity-modulated radiation treatment, which results in increased beam-on time and therefore in more scatter radiation to a larger area of the body, has led to speculation that it may result in a higher frequency of second cancers than occurs after conventional radiation therapy (*73–75*). The challenge for the future is to identify cohorts of patients and develop dosimetry resources necessary to understand the long-term effects of new diagnostic and treatment modalities.

[5] C. R. Blackwell, D. H. Novack and M. Stovall, unpublished data.

APPENDIX

TABLE A1
Epidemiological Studies of Medical Irradiation with Reconstruction of Individual Organ Doses

Modality	Dose reconstruction organ site	Mean organ dose, Gy (range)	Dosimetry method	Number of patients[a]	Reference(s)
1. Patients receiving high-dose radiation therapy for malignant diseases					
1.1 Breast cancer					
External beam	Contralateral breast	3.02 (maximum 7.1) for cases 2.67 for controls 2.82 total (maximum 7.1)	2: Construction of special phantom	Cases = 655 Controls = 1189	Boice *et al.* (*76*)
External beam	Contralateral breast	2.51 (0.52–4.6)	2: Construction of special phantom	Cases = 529 Controls = 529	Storm *et al.* (*77*)
External beam	Bone marrow	5.3 (1.3–10)	2: Dose estimated to 16 bone marrow components	Cases = 48 Controls = 97	Curtis *et al.* (*78*)
External beam	Bone marrow	7.5 (<5.0–9.0+)	1, 2: Dose estimated to 16 bone marrow components	Cases = 90 Controls = 264	Curtis *et al.* (*79*)
External beam	Lung (ipsilateral) Lung (contralateral) Lung (both)	15.2 4.6 9.8	1 1 1	Cases = 61 Controls = 120	Inskip *et al.* (*80*)
1.2 Cervical cancer					
External beam Brachytherapy	Bone marrow	7.2 (1–25)	1, 2, 4: Dose estimated to 14 bone marrow components	Cases = 195 Controls = 745	Boice *et al.* (*45*)
External beam Brachytherapy	20 different organs	Varied by site (0.1–60)	1, 2, 4	Cases = 4188 Controls = 6880	Boice *et al.* (*44*, *46*) Stovall *et al.* (*19*)
External beam Brachytherapy	Breast	0.31 (0.1–0.98)	1, 2	Cases = 953 Controls = 1806	Boice *et al.* (*81*)
1.3 Hodgkin lymphoma					
External beam	Lung	(0.5–4.9)	1 (with correction for lung blocking)	Cases = 98 Controls = 259	Kaldor *et al.* (*82*)
External beam	Lung	7.2 (<1–15.2) cases 6.7 (<1–21.0) controls	1, 3	Cases = 29 Controls = 82	van Leeuwen *et al.* (*83*)
External beam	Lung	27.2 (median 33.8) cases 21.8 (median 29.4) controls	1, 3	Cases = 222 Controls = 444 Cases = 227 Controls = 455	Travis *et al.* (*41*) Gilbert *et al.* (*42*)
External beam	Breast	25.1 (12–61.3) cases	1, 3: Review of simulation films, CT images, and radiographs to locate 2nd tumor	Cases = 105 Controls = 266	Travis *et al.* (*49*)
		21.1 (<0.1–56) controls		Cases = 48 Controls = 175	van Leeuwen *et al.* (*84*)
External beam	Bone marrow	<10–>20 same range for cases and controls	1	Cases = 163 Controls = 455	Kaldor *et al.* (*85*)
1.4 Non-Hodgkin lymphoma					
External beam	Bladder	12.9 (median) cases 20.4 (median) controls	1	Cases = 31 Controls = 89	Travis *et al.* (*86*)
	Kidney	12.8 (median) (4.2–45) cases 4.8 (median) (1.6–10.9) controls		Cases = 17 Controls = 47	
External beam	Bone marrow	9.3 (median) (15.2 with chemotherapy) 5.1 (median) (8.6 with chemotherapy)	1	Cases = 35 Controls = 140	Travis *et al.* (*87*)
External beam	Bone marrow	5.2 (median) (1.1–20.7)	1	Cohort = 61	Travis *et al.* (*88*)
1.5 Ovarian cancer					
External beam	Bone marrow	18.4	1	Cases = 114 Controls = 342	Kaldor *et al.* (*89*)
				Cases = 96 Controls = 272	Travis *et al.* (*90*)
External beam Brachytherapy	Bladder	40 (median)	1, 4	Cases = 63 Controls = 188	Kaldor *et al.* (*91*)
1.6 Testicular cancer					
External beam	Bone marrow	13.6 (8.6–23.8) 12.3 (7.9–22.9)	1	Cases = 36 Controls = 106	Travis *et al.* (*92*)
1.7 Uterine cancer					
External beam Brachytherapy	Bone marrow	5.2 for both modalities 1.7 (0.7–2.7) for brachytherapy 9.7 (6.4–14) for external beam	1, 4	Cases = 218 Controls = 775	Curtis *et al.* (*93*)

(Continued on page 153)

TABLE A1
Continued

Modality	Dose reconstruction organ site	Mean organ dose, Gy (range)	Dosimetry method	Number of patients[a]	Reference(s)
1.8 Retinoblastoma					
External beam	Bone	32.8 (0–193)	1	Cases = 52	Wong *et al.* (*43*)
Brachytherapy		20.0 (0–212)		Controls = 89	
	Soft tissue	20.4 (0–82.1)		Cases = 31	
		10.6 (0–112)		Controls = 89	
1.9 Childhood cancer					
External beam	Bone	16.9 (<19–60+)	1, 2	Cases = 64 Controls = 209	Tucker *et al.* (*94*)
External beam	Bone marrow	10.0 (0–38.0)	1	Cases = 25 Controls = 90	Tucker *et al.* (*95*)
External beam	Bone marrow	(0–1.5)	1	Cases = 26 Controls = 96	Hawkins *et al.* (*96*)
External beam	Bone	(0.08–75.7) (0.1–55.2)	1, 2	Cases = 59 Controls = 220	Hawkins *et al.* (*97*)
External beam	Thyroid	12.5 (0–76) 3.6 median	1, 2	Cases = 23 Controls = 89	Tucker *et al.* (*98*)
		2. Patients receiving moderate to high-dose radiation therapy for benign conditions			
2.1 Infertility (USA)					
External beam	Ovary	0.9 (0.6–1.5)	1, 2	Cohort = 816	Ron *et al.* (*99*)
	Brain	0.6 (0.001–1.2)			
	Uterus	0.5 (0.04–0.9)			
	Colon	0.5 (0.4–0.9)			
	Bone marrow	0.3 (0.2–0.5)			
	Thyroid	0.03 (0.002–0.2)			
	Breast	0.1 (0.007–0.01)			
2.2 Infertility (Israel)					
External beam	Brain	0.8 (0.6–1.1)	1, 2	Cohort = 968	Ron *et al.* (*100*)
	Colon	0.6 (0.001–0.8)		Doses based on a sample of 633 women	
	Ovary	1.0 (0.001–1.4)			
	Bone marrow	0.4 (0.1–0.4)			
2.3 Nasopharyngeal radiation in childhood					
Brachytherapy	Pituitary	10.9 (1–59)	2, 4: Radium applicators	Cohort = 8443	Ronckers *et al.* (*101–103*)
	Tongue, base	20.7 (2–130)	15% correction for monel filtration		
	Parotid gland	7.0 (1–28)			
	Brain	1.8 (0.3–8.0)			
	Thyroid	1.5 (0.2–11)			
2.4 Tonsil irradiation in childhood (Chicago)					
External beam	Thyroid	5.9 (4.4–7.0)	1, 2	Cohort = 4296	Schneider *et al.* (*35–37*)
	Salivary gland	4.2 (0.02–15.8)			
	Parathyroid	0.77 (0.3–1.0) cases 0.58 cohort			
2.5 Tonsil irradiation in childhood (Boston)					
External beam	Thyroid	0.24 (0.03–0.55)	1, 2	Cohort = 2258	Pottern *et al.* (*104*)
2.6 Benign gynecologic disease					
Brachytherapy	Bone marrow	0.53 (0.26–0.85)	1, 2, 4	Cohort = 4483	Inskip (*105*)
External beam		1.30 (0.06–2.0)			
		0.21 (0.11–0.34)			
2.7 Tinea Capitis (Israel)					
External beam	Thyroid	0.09 (0.04–0.49)	2: New dosimetry based on earlier experimental measurements	Cohort = 10,834	Ron *et al.* (*31, 32, 106*)
	Brain	1.5 (1.0–6.0)			
	Scalp	6.8 (5.5–24.4)			
2.8 Peptic ulcer					
External beam	Stomach	14.8	1, 2: Original radiotherapist verified treatment parameters, measurements made on original machines	Cohort = 3609	Griem *et al.* (*38*) Carr *et al.* (*39–40*)
	Pancreas	12.9			
	Lung	1.8			
	Heart	2.1			

(Continued on page 154)

TABLE A1
Continued

Modality	Dose reconstruction organ site	Mean organ dose, Gy (range)	Dosimetry method	Number of patients[a]	Reference(s)
		3. Patients receiving protracted or fractionated diagnostic radiation			
3.1 Scoliosis					
Repeated diagnostic X rays	Breast	0.11 (0–1.7)	5: Detailed information on 25% of cohort. Used standard software to estimate doses.	Cohort = 5573	Doody *et al.* (*47*)
3.2 Leukemia, lymphoma, and multiple myeloma following diagnostic X rays					
Repeated diagnostic X rays	Bone marrow	(0–0.23)	Bone marrow dose assigned to each X-ray procedure based on extensive literature search	Cases = 1091 Controls = 1390	Boice *et al.* (*107*)

Notes. Method: 1 = water phantom and mathematical calculation; 2 = anthropomorphic phantom; 3 = treatment planning; 4 = brachythrapy (isodose curves); 5 = diagnostic radiation (standard software).

[a] Number of patients for specific analyses may vary due to missing dose or other information.

ACKNOWLEDGMENTS

This work was supported in part by Contract NO1-CP-91024 from the National Cancer Institute, NIH, DHHS. The authors would like to thank Dr. Steve Simon for his helpful comments.

REFERENCES

1. M. P. Little, Comparison of the risks of cancer incidence and mortality following radiation therapy for benign and malignant disease with the cancer risks observed in the Japanese A-bomb survivors. *Int. J. Radiat. Biol.* **77**, 431–464 (2001).
2. United Nations Scientific Committee on the Effects of Atomic Radiation, *Sources and Effects of Ionizing Radiation*, Vol. I: *Sources*; Vol. II: *Effects*, UNSCEAR 2000 report to the General Assembly, with Scientific Annexes. E.00.IX.4, United Nations, New York, 2000.
3. IARC, *Ionizing Radiation*, Part 1: *X- and Gamma (γ)-Radiation, and Neutrons. IARC Monographs on the Evaluation of the Carcinogenic Risks to Humans*, Vol. 75, International Agency for Research on Cancer, Lyon, 2000.
4. W. Snyder, M. Ford, G. Warner and S. Watson, *"S," Absorbed Dose Per Unit Cumulated Activity for Selected Radionuclides and Organs*. MIRD Pamphlet No. 11, Society of Nuclear Medicine, New York, 1975.
5. M. Stovall, S. S. Donaldson, R. E. Weathers, L. L. Robison, A. C. Mertens, J. F. Winther, J. H. Olsen and J. D. Boice, Jr., Genetic effects of radiotherapy for childhood cancer: Gonadal dose reconstruction. *Int. J. Radiat. Oncol. Biol. Phys.* **60**, 542–552 (2004).
6. M. Stovall, C. R. Blackwell, J. Cundiff, D. H. Novack, J. R. Palta, L. K. Wagner, E. W. Webster and R. J. Shalek, Fetal dose from radiotherapy with photon beams: Report of AAPM Radiation Therapy Committee Task Group No. 36. *Med. Phys.* **22**, 63–82 (1995).
7. M. Stovall, C. R. Blackwell, J. Cundiff, D. H. Novack, J. R. Palta, L. K. Wagner, E. W. Webster and R. J. Shalek, Fetal dose from radiotherapy with photon beams: report of AAPM Radiation Therapy Committee Task Group No. 36. *Med. Phys.* **22**, 63–82 (1995); Erratum, *Med. Phys.* **22,** 1353–1354 (1995).
8. E. G. A. Aird, J. E. Burns, M. J. Day, S. Duane, T. J. Jordan, A. Kacperek, S. C. Klevenhagen, R. M. Harrison, S. C. Lillicrap and C. W. Smith, Central axis depth dose data for use in radiation therapy: 1996, A survey of depth doses and related data measured in water or equivalent media. *Br. J. Radiol.* Suppl. 25 (1996).
9. R. G. Snyder, L. W. Schneider, C. L. Owings, H. M. Reynolds, D. H. Golomb and M. A. Schork, *Anthropometry of Infants, Children, and Youths to Age 18 for Product Safety Design SP450*. Society of Automotive Engineers, Warrendale, PA, 1977.
10. C. Eycleshymer and D. M. Schoemaker, *A Cross-Section Anatomy*. Appleton-Century-Crofts, New York, 1970.
11. S. A. Kieffer and E. R. Heitzman, Eds., *An Atlas of Cross-Sectional Anatomy*. Harper & Row, Hagerstown, MD, 1979.
12. H. Ferner and J. Staubesand, Eds., *Sobotta Atlas of Human Anatomy, Vol. 1: Head, Neck, Upper Extremities*, 10th English ed. Urban & Schwarzenberg, Baltimore, 1983.
13. H. Ferner and J. Staubesand, Eds., *Sobotta Atlas of Human Anatomy, Vol. 2: Thorax, Abdomen, Pelvis, Lower Extremities, Skin*, 10th English ed. Urban & Schwarzenberg, Baltimore, 1983.
14. W. J. Bo, N. T. Wolfman, W. A. Krueger, J. J. Carr, R. L. Bowden and I. Meschan, *Basic Atlas of Sectional Anatomy with Correlated Imaging*. W. B. Saunders, Philadelphia, 1998.
15. M. Cristy, *Mathematical Phantoms Representing Children of Various Ages for Use in Estimates of Internal Dose*. Report ORNL/NUREG/TM 367, Oak Ridge National Laboratory Oak Ridge, TN, 1980.
16. M. Cristy, Active bone marrow distribution as a function of age in humans. *Phys. Med. Biol.* **26**, 389–400 (1981).
17. R. J. Shalek and M. Stovall, The M. D. Anderson method for the computation of isodose curves around interstitial and intracavitary radiation sources. I. Dose from linear sources. *Am. J. Roentgenol. Radiat. Ther. Nuclear Med.* **102**, 662–672 (1968).
18. R. J. Shalek and M. Stovall, Brachytherapy dosimetry. In *The Dosimetry of Ionizing Radiation*, Vol. III (K. Kase, B. E. Bjarngard and F. H. Attix, Eds.), pp. 259–321. Academic Press, San Diego, 1990.
19. M. Stovall, S. A. Smith and M. Rosenstein, Tissue doses from radiotherapy of cancer of the uterine cervix. *Med. Phys.* **16**, 726–733 (1989).
20. K. L. Bontrager, *Pocket Handbook, Radiographic Positioning and Techniques*. Botanger Publishing, Peoria, IL, 1985.
21. C. A. Dennis, C. R. May and R. L. Eisenberg, *Radiographic Positioning Pocket Manual*. Little, Brown and Company, Boston, 1995.
22. M. Rosenstein, *Handbook of Selected Organ Doses for Projections Common in Diagnostic Radiology*. FDA Publication 76-8031, U.S. Dept. of Health, Education, Welfare, Public Health Service, Rockville, MD, 1976.
23. M. Rosenstein, T. J. Beck and G. G. Warner, *Handbook of Selected Organ Doses for Projections Common in Pediatric Radiology*. FDA Publication 79-8079, U.S. Department of Health, Education, and Welfare, Public Health Service, Food and Drug Administration, Bureau of Radiological Health, Rockville, MD, 1979.
24. A. Werner, B. Modan and D. Davidoff, Doses to brain, skull and thyroid, following x-ray therapy for tinea capitis. *Phys. Med. Biol.* **13**, 247–258 (1968).

25. B. Modan, E. Ron and A. Werner, Thyroid cancer following scalp irradiation. *Radiology* **123**, 741–744 (1977).

26. N. H. Harley, R. E. Albert, R. E. Shore and B. S. Pasternack, Follow-up study of patients treated by x-ray epilation for tinea capitis. Estimation of the dose to the thyroid and pituitary glands and other structures of the head and neck. *Phys. Med. Biol.* **21**, 631–642 (1976).

27. R. J. Schulz and R. E. Albert, Follow-up study of patients treated by x-ray epilation for tinea capitis. 3. Dose to organs of the head from the x-ray treatment of tinea capitis. *Arch. Environ. Health* **17**, 935–950 (1968).

28. R. E. Shore, R. E. Albert and B. S. Pasternack, Follow-up study of patients treated by x-ray epilation for tinea capitis; Resurvey of post-treatment illness and mortality experience. *Arch. Environ. Health* **31**, 21–28 (1976).

29. H. G. Adamson, A simplified method of x-ray application for the cure of ringworm of the scalp: Kienboch's method. *Lancet* **1**, 1378–1380, 1909.

30. W. Lee and H. D. Youmans, Doses to the central nervous system resulting from x-ray therapy for tinea capitis. Publication No. BRH/DBE 70-4, Bureau of Radiological Health, U.S. FDA, Washington, DC, 1970.

31. E. Ron, B. Modan, J. D. Boice, Jr., E. Alfandary, M. Stovall, A. Chetrit and L. Katz, Tumors of the brain and nervous system after radiotherapy in childhood. *N. Engl. J. Med.* **319**, 1033–1039 (1988).

32. E. Ron, B. Modan, D. Preston, E. Alfandary, M. Stovall and J. D. Boice, Jr., Thyroid neoplasia following low-dose radiation in childhood. *Radiat. Res.* **120**, 516–531 (1989).

33. D. W. Schafer, J. H. Lubin, E. Ron, M. Stovall and R. J. Carroll, Thyroid cancer following scalp irradiation: a reanalysis accounting for uncertainty in dosimetry. *Biometrics* **57**, 689–697 (2001).

34. J. H. Lubin, D. W. Schafer, E. Ron, M. Stovall and R. J. Carroll, A reanalysis of thyroid neoplasms in the Israeli tinea capitis study accounting for dose uncertainties. *Radiat. Res.* **161**, 359–368 (2004).

35. A. B. Schneider, E. Ron, J. Lubin, M. Stovall and T. C. Gierlowski, Dose–response relationships for radiation-induced thyroid cancer and thyroid nodules: Evidence for the prolonged effects of radiation on the thyroid. *J. Clin. Endocrinol. Metab.* **77**, 362–369 (1993).

36. A. B. Schneider, T. C. Gierlowski, E. Shore-Freedman, M. Stovall, E. Ron and J. Lubin, Dose–response relationships for radiation-induced hyperparathyroidism. *J. Clin. Endocrinol. Metab.* **80**, 254–257 (1995).

37. A. B. Schneider, J. Lubin, E. Ron, C. Abrahams, M. Stovall, A. Goel, E. Shore-Freedman and T. C. Gierlowski, Salivary gland tumors after childhood radiation treatment for benign conditions of the head and neck: Dose–response relationships. *Radiat. Res.* **149**, 625–630 (1998).

38. M. L. Griem, R. A. Kleinerman, J. D. Boice, Jr., M. Stovall, D. Shefner and J. H. Lubin, Cancer following radiotherapy for peptic ulcer. *J. Natl. Cancer Inst.* **86**, 842–849 (1994).

39. Z. A. Carr, R. A. Kleinerman, M. Stovall, R. M. Weinstock, M. L. Griem and C. E. Land, Malignant neoplasms after radiation therapy for peptic ulcer. *Radiat. Res.* **157**, 668–677 (2002).

40. Z. A. Carr, C. E. Land, R. A. Kleinerman, R. W. Weinstock, M. Stovall, M. L. Griem and K. Mabuchi, Coronary heart disease after radiotherapy for peptic ulcer disease. *Int. J. Radiat. Oncol. Biol. Phys.* **61**, 842–851 (2005).

41. L. B. Travis, M. Gospodarowicz, R. E. Curtis, E. A. Clarke, M. Andersson, B. Glimelius, T. Joensuu, C. F. Lynch, F. E. van Leeuwen and E. Gilbert, Lung cancer following chemotherapy and radiotherapy for Hodgkin's disease. *J. Natl. Cancer Inst.* **94**, 182–192 (2002).

42. E. S. Gilbert, M. Stovall, M. Gospodarowicz, F. E. van Leeuwen, M. Andersson, B. Glimelius, T. Joensuu, C. F. Lynch, R. E. Curtis and L. B. Travis, Lung cancer after treatment for Hodgkin's disease: Focus on radiation effects. *Radiat. Res.* **159**, 161–173 (2003).

43. F. L. Wong, J. D. Boice, Jr., D. H. Abramson, R. E. Tarone, R. A. Kleinerman, M. Stovall, M. B. Goldman, J. M. Seddon, N. Tarbell and F. P. Li, Cancer incidence after retinoblastoma. Radiation dose and sarcoma risk. *J. Am. Med. Assoc.* **278**, 1262–1267 (1997).

44. J. D. Boice, Jr., N. E. Day, A. Andersen, L. A. Brinton, R. Brown, N. W. Choi, E. A. Clarke, M. P. Coleman, R. E. Curtis and C. Wall, Second cancers following radiation treatment for cervical cancer. An international collaboration among cancer registries. *J. Natl. Cancer Inst.* **74**, 955–975 (1985).

45. J. D. Boice, Jr., M. Blettner, R. A. Kleinerman, M. Stovall, W. C. Moloney, G. Engholm, D. F. Austin, A. Bosch, D. L. Cookfair and G. B. Hutchinson, Radiation dose and leukemia risk in patients treated for cancer of the cervix. *J. Natl. Cancer Inst.* **79**, 1295–1311 (1987).

46. J. D. Boice, Jr., G. Engholm, R. A. Kleinerman, M. Blettner, M. Stovall, H. Lisco, W. C. Moloney, D. F. Austin, A. Bosch and B. MacMahon, Radiation dose and second cancer risk in patients treated for cancer of the cervix. *Radiat. Res.* **116**, 3–55 (1988).

47. M. M. Doody, J. E. Lonstein, M. Stovall, D. G. Hacker, N. Luckyanov and C. E. Land, Breast cancer mortality after diagnostic radiography: Findings from the U.S. Scoliosis Cohort Study. *Spine* **25**, 2052–2063 (2000).

48. ICRU, *Determination of Absorbed Dose in a Patient Irradiated by Beams of X or Gamma Rays in Radiation Therapy Procedures.* Report 24, International Commission on Radiation Units and Measurements, Washington, DC, 1976.

49. L. B. Travis, D. A. Hill, G. M. Dores, M. Gospodarowicz, F. E. van Leeuwen, E. Holowaty, B. Glimelius, M. Andersson, T. Wiklund and E. Gilbert, Breast cancer following radiotherapy and chemotherapy among young women with Hodgkin disease. *J. Am. Med. Assoc.* **290**, 465–475 (2003).

50. B. A. Fraass and J. van de Geijn, Peripheral dose from megavolt beams. *Med. Phys.* **10**, 809–818 (1983).

51. K. R. Kase, G. K. Svensson, A. B. Wolbarst and M. A. Marks, Measurements of dose from secondary radiation outside a treatment field. *Int. J. Radiat. Oncol. Biol. Phys.* **9**, 1177–1183 (1983).

52. D. Greene, G. L. Chu and D. W. Thomas, Dose levels outside radiotherapy beams. *Br. J. Radiol.* **56**, 543–550 (1983).

53. D. Greene, P. G. Karup, C. Sims and R. J. Taylor, Dose levels outside radiotherapy beams. *Br. J. Radiol.* **58**, 453–456 (1985).

54. P-H. Van der Giessen and H. W. J. Bierhuizen, Comparison of measured and calculated peripheral doses in patients undergoing radiation therapy. *Radiother. Oncol.* **42**, 265–270 (1997).

55. P-H. Van der Giessen, A simple and generally applicable method to estimate the peripheral dose in radiation teletherapy with high energy x-rays or gamma radiation. *Int. J. Radiat. Oncol. Biol. Phys.* **35**, 1059–1068 (1996).

56. P. François, C. Beurtheret, A. Dutreix and F. DeVathaire, A mathematical child phantom for the calculation of dose to the organs at risk. *Med. Phys.* **15**, 328–333 (1988).

57. P. François, C. Beurtheret and A. Dutreix, Calculation of the dose delivered to organs outside the radiation beams. *Med. Phys.* **15**, 879–883 (1988).

58. J. D. Boice, Jr., M. Rosenstein and E. D. Trout, Estimation of breast doses and breast cancer risk associated with repeated fluoroscopic chest examinations of women with tuberculosis. *Radiat. Res.* **73**, 373–390 (1978).

59. W. M. Court-Brown and R. Doll, Leukaemia and aplastic anaemia in patients treated for ankylosing spondylitis. *Spec. Rep. Ser. Med. Res. Counc. (C.-B.)* 1–135 (1957).

60. F. de Vathaire, M. Hawkins, S. Campbell, O. Oberlin, M. A. Raquin, J. Y. Schlienger, A. Shamsaldin, I. Diallo, J. Bell and J. Lemerle, Second malignant neoplasms after a first cancer in childhood: Temporal pattern of risk according to type of treatment. *Br. J. Cancer* **79**, 1884–1893 (1999).

61. F. de Vathaire, C. Hardiman, A. Shamsaldin, S. Campbell, E. Grimaud, M. Hawkins, M. Raquin, O. Oberlin, I. Diallo and C. Bonaiti, Thyroid carcinomas after irradiation for a first cancer during childhood. *Arch. Intern. Med.* **159**, 2713–2719 (1999).

62. N. H. Harley, R. E. Albert, R. E. Shore and B. S. Pasternack, Fol-

low-up study of patients treated by x-ray epilation for tinea capitis. Estimation of the dose to the thyroid and pituitary glands and other structures of the head and neck. *Phys. Med. Biol.* **21**, 631–642 (1976).

63. N. G. Hildreth, R. E. Shore, L. H. Hempelmann and M. Rosenstein, Risk of extra-thyroid tumors following radiation treatment in infancy for thymic enlargement. *Radiat. Res.* **102**, 378–391 (1985).

64. L. Johansson, L. G. Larsson and L. Damber, A cohort study with regard to the risk of haematological malignancies in patients treated with x-rays for benign lesions in the locomotor system. II. Estimation of absorbed dose in the red bone marrow. *Acta Oncol.* **34**, 721–726 (1995).

65. C. A. Lewis, P. G. Smith, I. M. Stratton, S. C. Darby and R. Doll, Estimated radiation doses to different organs among patients treated for ankylosing spondylitis with a single course of X rays. *Br. J. Radiol.* **61**, 212–220 (1988).

66. M. Lundell, Estimates of absorbed dose in different organs in children treated with radium for skin hemangiomas. *Radiat. Res.* **140**, 327–333 (1994).

67. A. Mattsson, B. I. Ruden, P. Hall, N. Wilking and L. E. Rutqvist, Radiation-induced breast cancer: Long-term follow-up of radiation therapy for benign breast disease. *J. Natl. Cancer Inst.* **85**, 1679–1685 (1993).

68. R. J. Schulz and R. E. Albert, Follow-up study of patients treated by x-ray epilation for tinea capitis. 3. Dose to organs of the head from the x-ray treatment of tinea capitis. *Arch. Environ. Health* **17**, 935–950 (1968).

69. H. A. Weiss, S. C. Darby and R. Doll, Cancer mortality following X-ray treatment for ankylosing spondylitis. *Int. J. Cancer* **59**, 327–338 (1994).

70. E. Ron and F. O. Hoffman, Eds., *Uncertainties in Radiation Dosimetry and Their Impact on Dose–Response Analyses.* NIH Publication no. 99-4541, National Cancer Institute, National Institutes of Health, Public Health Service, DHHS, Bethesda, MD, 1999.

71. D. J. Brenner, C. Elliston, E. Hall and W. Berdon, Estimated risks of radiation-induced fatal cancer from pediatric CT. *Am. J. Roentgenol.* **176**, 289–296 (2001).

72. D. J. Brenner and C. D. Elliston, Estimated radiation risks potentially associated with full-body CT screening. *Radiology* **232**, 735–738 (2004).

73. D. Followill, P. Geis and A. Boyer, Estimates of whole-body dose equivalent produced by beam intensity modulated conformal therapy. *Int. J. Radiat. Oncol. Biol. Phys.* **38**, 667–672 (1997).

74. S. Mutic, J. Esthappan and E. E. Klein, Peripheral dose distributions for a linear accelerator equipped with a secondary multileaf collimator and universal wedge. *J. Appl. Clin. Med. Phys.* **3**, 302–309 (2002).

75. E. J. Hall and C. S. Wuu, Radiation-induced second cancers: The impact of 3D-CRT and IMRT. *Int. J. Radiat. Oncol. Biol. Phys.* **56**, 83–88 (2003).

76. J. D. Boice, Jr., E. B. Harvey, M. Blettner, M. Stovall and J. T. Flannery, Cancer in the contralateral breast after radiotherapy for breast cancer. *N. Engl. J. Med.* **326**, 781–785 (1992).

77. H. Storm, M. Andersson, J. D. Boice, Jr., M. Blettner, M. Stovall, H. T. Mouridsen, P. Dombernowsky, C. Rose, A. Jacobsen and M. Pedersen, Adjuvant radiotherapy and risk of contralateral breast cancer. *J. Natl. Cancer Inst.* **84**, 1245–1250 (1992).

78. R. E. Curtis, J. D. Boice, Jr., M. Stovall, J. T. Flannery and W. C. Moloney, Leukemia risk following radiotherapy for breast cancer. *J. Clin. Oncol.* **7**, 21–29 (1989).

79. R. E. Curtis, J. D. Boice, Jr., M. Stovall, L. Bernstein, R. S. Greenberg, J. T. Flannery, A. G. Schwartz, P. Weyer, W. C. Moloney and R. N. Hoover, Risk of leukemia after chemotherapy and radiation treatment for breast cancer. *N. Engl. J. Med.* **326**, 1745–1751 (1992).

80. P. D. Inskip, M. Stovall and J. T. Flannery, Lung cancer risk and radiation dose among women treated for breast cancer. *J. Natl. Cancer Inst.* **86**, 983–988 (1994).

81. J. D. Boice, Jr., M. Blettner, R. A. Kleinerman, G. Engholm, M. Stovall, H. Lisco, D. F. Austin, A. Bosch, L. Harlan and B. MacMahon, Radiation dose and breast cancer risk in patients treated for cancer of the cervix. *Int. J. Cancer* **44**, 7–16 (1989).

82. J. M. Kaldor, N. E. Day, J. Bell, E. A. Clarke, F. Langmark, S. Karjalainen, P. Band, D. Pedersen, W. Choi and M. Stovall, Lung cancer following Hodgkin's disease: A case-control study. *Int. J. Cancer* **52**, 677–681 (1992).

83. F. E. van Leeuwen, W. J. Klokman, M. Stovall, A. Hagenbeek, A. W. van den Belt-Dusebout, R. Noyon, J. D. Boice, Jr., J. M. Burgers and R. Somers, Roles of radiotherapy and smoking in lung cancer following Hodgkin's disease. *J. Natl. Cancer Inst.* **87**, 1530–1537 (1995).

84. F. E. van Leeuwen, W. J. Klokman, M. Stovall, E. C. Dahler, M. B. van't Veer, E. M. Noordijk, M. A. Crommelin, B. M. Aleman and N. S. Russell, Roles of radiation dose, chemotherapy, and hormonal factors in breast cancer following Hodgkin's disease. *J. Natl. Cancer Inst.* **95**, 971–980 (2003).

85. J. M. Kaldor, N. E. Day, E. A. Clarke, F. E. van Leeuwen, M. Henry-Amar, M. V. Fiorentino, J. Bell, D. Pedersen, P. Band and M. Stovall, Leukemia following Hodgkin's disease. *N. Engl. J. Med.* **322**, 7–13 (1990).

86. L. B. Travis, R. E. Curtis, B. Glimelius, E. J. Holowaty, F. E. van Leeuwen, C. F. Lynch, A. Hagenbeek, M. Stovall, P. M. Banks and J. D. Boice, Jr., Bladder and kidney cancer following cyclophosphamide therapy for non-Hodgkin's lymphoma. *J. Natl. Cancer Inst.* **87**, 524–530 (1995).

87. L. B. Travis, R. E. Curtis, M. Stovall, E. J. Holowaty, F. E. van Leeuwen, B. Glimelius, C. F. Lynch, A. Hagenbeek, C. Y. Li and J. D. Boice, Jr., Risk of leukemia following treatment for non-Hodgkin's lymphoma. *J. Natl. Cancer Inst.* **86**, 1450–1457 (1994).

88. L. B. Travis, J. Weeks, R. E. Curtis, J. T. Chaffey, M. Stovall, P. M. Banks and J. D. Boice, Jr., Leukemia following low-dose total body irradiation and chemotherapy for non-Hodgkin's lymphoma. *J. Clin. Oncol.* **14**, 565–571 (1996).

89. J. M. Kaldor, N. E. Day, F. Pettersson, E. A. Clarke, D. Pedersen, W. Mehnert, J. Bell, H. Host, P. Prior and M. Stovall, Leukemia following chemotherapy for ovarian cancer. *N. Engl. J. Med.* **322**, 1–6 (1990).

90. L. B. Travis, E. J. Holowaty, K. Bergfeldt, C. F. Lynch, B. A. Kohler, T. Wiklund, R. E. Curtis, P. Hall, M. Andersson and M. Stovall, Risk of leukemia after platinum-based chemotherapy for ovarian cancer. *N. Engl. J. Med.* **340**, 351–357 (1999).

91. J. M. Kaldor, N. E. Day, B. Kittelmann, F. Pettersson, F. Langmark, D. Pedersen, P. Prior, F. Neal, S. Karjalainen and P. Boffetta, Bladder tumours following chemotherapy and radiotherapy for ovarian cancer: A case-control study. *Int. J. Cancer* **63**, 1–6 (1995).

92. L. B. Travis, M. Andersson, M. Gospodarowicz, F. E. van Leeuwen, K. Bergfeldt, C. F. Lynch, R. E. Curtis, B. A. Kohler, T. Wiklund and E. Gilbert, Treatment-associated leukemia following testicular cancer. *J. Natl. Cancer Inst.* **92**, 1165–1171 (2000).

93. R. E. Curtis, J. D. Boice, Jr., M. Stovall, L. Bernstein, E. Holowaty, S. Karjalainen, F. Langmark, P. C. Nasca, A. G. Schwartz and W. C. Maloney, Relationship of leukemia risk to radiation dose following cancer of the uterine corpus. *J. Natl. Cancer Inst.* **86**, 1315–1324 (1994).

94. M. A. Tucker, G. J. D'Angio, J. D. Boice, Jr., L. C. Strong, F. P. Li, M. Stovall, B. J. Stone, D. M. Green, F. Lombardi and G. B. Hutchinson, Bone sarcomas linked to radiotherapy and chemotherapy in children. *N. Engl. J. Med.* **317**, 588–593 (1987).

95. M. A. Tucker, A. T. Meadows, J. D. Boice, Jr., M. Stovall, O. Oberlin, B. J. Stone, J. Birch, P. A. Voute, R. N. Hoover and J. F. Fraumeni, Jr., Leukemia after therapy with alkylating agents for childhood cancer. *J. Natl. Cancer Inst.* **78**, 459–464 (1987).

96. M. M. Hawkins, L. M. Wilson, M. A. Stovall, H. B. Marsden, M. H. Potok, J. E. Kingston and J. M. Chessells, Epipodophyllotoxins, alkylating agents, and radiation and risk of secondary leukaemia after childhood cancer. *Br. Med. J.* **304**, 951–958 (1992).

97. M. M. Hawkins, L. M. Wilson, H. S. Burton, M. H. Potok, D. L.

Winter, H. B. Marsden and M. A. Stovall, Radiotherapy, alkylating agents, and risk of bone cancer after childhood cancer. *J. Natl. Cancer Inst.* **88**, 270–278 (1996).

98. M. A. Tucker, P. H. Jones, J. D. Boice, Jr., L. L. Robison, B. J. Stone, M. Stovall, R. D. Jenkin, J. H. Lubin, E. S. Baum and J. F. Fraumeni, Jr., Therapeutic radiation at a young age is linked to secondary thyroid cancer. The Late Effects Study Group. *Cancer Res.* **51**, 2885–2888 (1991).

99. E. Ron, J. D. Boice, Jr., S. Hamburger and M. Stovall, Mortality following radiation treatment for infertility of hormonal origin or amenorrhoea. *Int. J. Epidemiol.* **23**, 1165–1173 (1994).

100. E. Ron, A. Auvinen, E. Alfandary, M. Stovall, B. Modan and A. Werner, Cancer risk following radiotherapy for infertility or menstrual disorders. *Int. J. Cancer* **82**, 795–798 (1999).

101. C. M. Ronckers, C. E. Land, P. G. Verduijn, R. B. Hayes, M. Stovall and F. E. van Leeuwen, Cancer mortality after nasopharyngeal radium irradiation in the Netherlands: A cohort study. *J. Natl. Cancer Inst.* **93**, 1021–1027 (2001).

102. C. M. Ronckers, C. E. Land, R. B. Hayes, P. G. Verduijn, M. Stovall and F. E. van Leeuwen, Late health effects of childhood nasopharyngeal radium irradiation: Nonmelanoma skin cancers, benign tumors, and hormonal disorders. *Pediatr. Res.* **52**, 850–858 (2002).

103. C. M. Ronckers, F. E. van Leeuwen, R. B. Hayes, P. G. Verduijn, M. Stovall and C. E. Land, Cancer incidence after nasopharyngeal radium irradiation. *Epidemiology* **13**, 552–560 (2002).

104. L. M. Pottern, M. M. Kaplan, P. R. Larsen, J. E. Silva, R. J. Koenig, J. H. Lubin, M. Stovall and J. D. Boice, Jr., Thyroid nodularity after childhood irradiation for lymphoid hyperplasia: A comparison of questionnaire and clinical findings. *J. Clin. Epidemiol.* **43**, 449–460 (1990).

105. P. D. Inskip, R. R. Monson, J. K. Wagoner, M. Stovall, F. G. Davis, R. A. Kleinerman and J. D. Boice, Jr., Leukemia following radiotherapy for uterine bleeding. *Radiat. Res.* **122**, 107–119 (1990).

106. E. Ron, B. Modan, D. Preston, E. Alfandary, M. Stovall and J. D. Boice, Jr., Radiation-induced skin carcinomas of the head and neck. *Radiat. Res.* **125**, 318–325 (1991).

107. J. D. Boice, Jr., M. M. Morin, A. G. Glass, G. D. Friedman, M. Stovall, R. N. Hoover and J. F. Fraumeni, Jr., Diagnostic x-ray procedures and risk of leukemia, lymphoma, and multiple myeloma. *J. Am. Med. Assoc.* **265**, 1290–1294 (1991).